PLANT SCIENCE TODAY
ISSN 2348-1900 (online)
Vol x(x): xx–xx
https://doi.org/10.14719/pst.3410

HORIZON
e-Publishing Group
HePG

RESEARCH ARTICLE

Nitric oxide inhibitory potential of *Curcuma angustifolia* Roxb. essential oil: An *in silico* and *in vitro* analysis

Ayushman Gadnayak, Ananya Nayak, Sudipta Jena, Ambika Sahoo, Pratap Chandra Panda, Asit Ray* & Sanghamitra Nayak*

Centre for Biotechnology, Siksha 'O' Anusandhan (Deemed to be University), Bhubaneswar-751 003, India

*Email: asitray2007@gmail.com; sanghamitranayak@soa.ac.in

OPEN ACCESS

ARTICLE HISTORY

Received: 19 February 2024
Accepted: 16 July 2024

Available online
Version 1.0 : 28 September 2024

Check for updates

Additional information

Peer review: Publisher thanks Sectional Editor and the other anonymous reviewers for their contribution to the peer review of this work.

Reprints & permissions information is available at https://horizonepublishing.com/journals/index.php/PST/open_access_policy

Publisher's Note: Horizon e-Publishing Group remains neutral with regard to jurisdictional claims in published maps and institutional affiliations.

Indexing: Plant Science Today, published by Horizon e-Publishing Group, is covered by Scopus, Web of Science, BIOSIS Previews, Clarivate Analytics, NAAS, UGC Care, etc See https://horizonepublishing.com/journals/index.php/PST/indexing_abstracting

CITE THIS ARTICLE

Gadnayak A, Nayak A, Jena S, Sahoo A, Panda PC, Ray A, Nayak S. Nitric oxide inhibitory potential of *Curcuma angustifolia* Roxb. essential oil: An *in silico* and *in vitro* analysis. Plant Science Today (Early Access). https:/doi.org/10.14719/pst.3410

Abstract

The essential oil (EO) derived from *Curcuma angustifolia* Roxb. has gained significant interest in traditional medicine, specifically for its potential as a therapeutic agent for inflammatory disorders. Our study aimed to identify the chemical constituents of *C. angustifolia* EO, investigate its anti-inflammatory effects in lipopolysaccharide (LPS)-treated RAW 264.7 cells and explore potential nitric oxide (NO) inhibitors through *in silico* based studies. The essential oil obtained through hydro-distillation underwent analysis via gas chromatography-mass spectrometry (GC-MS). The major constituents were identified as velleral (17.82 %), germacrone (12.91 %), cryptomerione (11.52 %), curzerene (5.66 %) and β-elemene (4.09 %). The EO demonstrated non-toxicity up to a concentration of 50 µg/mL, maintaining over 70 % viability in RAW 264.7 cells. At a concentration of 25 µg/mL, treatment with *C. angustifolia* EO exhibited significant anti-inflammatory properties, leading to a 66 % decrease in LPS-induced NO production. Inducible nitric oxide synthase (iNOS) crystal structures were sourced from the RCSB database. Compounds identified through GC-MS analysis were retrieved from PubChem, docked by the molecular-docking process and tested for drug-likeness properties. The compounds such as velleral (-5.8 kcal/mol), germacrone (-5.4 kcal/mol), neocurdione (-5.2 kcal/mol) and γ-cadinene (-5.2 kcal/mol) exhibited the highest binding-affinity with iNOS. Molecular dynamics simulation (MDS) showed that the interaction of these 4 phyto-compounds was stable with the active site residues. Important bonds identified in the initial ligand-docked compounds persisted unaltered throughout the MDS. The present work with *in vitro* and *in silico* studies revealed that *C. angustifolia* EO could be a potential anti-inflammatory agent, thus necessitating further *in vivo* studies to develop promising therapeutic agents in the treatment of inflammation.

Keywords

Anti-inflammatory; *Curcuma angustifolia*; essential oil; *in vitro* analysis; iNOS; molecular docking; MD simulation; NO; RAW 264.7

Introduction

Inflammation often develops when infectious microbes, for example; bacteria, viruses or fungi, enter the body and circulate in the blood (1). Tissue injury, cell death, malignancy, ischemia and degeneration are among the additional pathologies that can trigger inflammation (1). While relying extensively on contemporary medicine and notable progress in synthetic drugs, 80 % of the global population adheres to traditional remedies derived directly from plant materials due to financial constraints or inability

to access products from the Western pharmaceutical industry (2). According to the World Health Organization, inflammation serves as the underlying factor for numerous non-communicable diseases, causing 41 million fatalities annually, which constitute 71 % of global deaths (3). Inflammation gives rise to various inflammatory mediators, including cytokines (such as interferons, tumor necrosis factor and interleukins), chemokines (such as eicosanoids like prostaglandins and leukotrienes), monocyte chemoattractant protein 1 and the influential inflammation-modulating transcription factor-nuclear factor B. These elements have been thoroughly investigated concerning human pathological conditions (1). Many diseases, like allergies, asthma, inflammatory bowel disease (IBD), rheumatoid arthritis and many more are caused by inflammation. Thus, clinicians are faced with a rising health problem and a difficult challenge in the form of dealing with these inflammatory diseases. Nitric oxide (NO) is a signalling molecule that plays an important role in the development of inflammation. It has an anti-inflammatory action under normal physiological conditions (4). However, in abnormal situations, NO is considered to be a pro-inflammatory mediator that causes inflammation. Nitric oxide synthase (NOS) is the primary contributor to reactive nitrogen/oxygen species synthesis in mammalian cells, particularly under certain pathological situations (5). NO is a potent pro-inflammatory compound produced during the inflammatory process. It promotes vasodilation and cellular migration while also down regulating adhesion molecules and causing inflammatory cell death (3).

The anti-inflammatory potential of plant essential oil and extracts has been documented since ancient times. Numerous reports on anti-inflammatory properties of essential oil have been published in recent decades (6, 7). This study deals with the anti-inflammatory activity of *Curcuma angustifolia* Roxb. rhizome essential oil (8). *C. angustifolia* essential oil has been used for a wide range of traditional remedies around the world (9). It is distributed in Asia, Africa and Australia. *C. angustifolia,* commonly known as East Indian Arrowroot, is commonly used in the central, eastern and southern regions of India (10, 11). Various Indian languages assign distinct names to *C. angustifolia*: Tikhur in Hindi, Tavakshira in Sanskrit, Keturi Halodhi in Bengali, Yaipan in Manipuri, Koova in Malayalam, Tavakeera in Marathi, Ararut-gaddalu in Telugu, Koove-hittu in Kannada and Ararut-kizhagu in Tamil (12). Tribes in Madhya Pradesh and Chhattisgarh utilize this plant to treat gastrointestinal disorders, bone fractures and inflammations (13). Tugak-sheeree, made from *C. angustifolia* starch, is a vital element in numerous Ayurvedic medicines (14). The essential oil extracted from the rhizomes of *C. angustifolia* has antifungal, antibacterial, anti-inflammatory, wound healing and anticancer properties (15, 16). This plant's starch is nutritious and easily absorbed and therefore has a wide range of potential medical applications. *C. angustifolia* oil has also been found to be effective in the treatment of colitis, peptic ulcers, dysentery, diarrhea etc (17). *C. angustifolia* is widely recommended for new born babies since it protects against infections, allergies and illness. It is also easy to digest, causing no constipation, diarrhea or upset stomach. *C. angustifolia* has major bioactive compounds such as Germacrone, Velleral, Neocurdione and Gamma-Cadinene, which act as anti-inflammatory agents (18). The essential oils are known for a variety of biological activities (19, 20). These also have a significant role in the development of modern medicine, along with Ayurvedic medicine (21).

The chemical composition and biological activity of *C. angustifolia* essential oil have not been investigated, despite its economic and medicinal importance. In the present study, we have analyzed the chemical composition of the essential oil derived from the rhizome of *C. angustifolia* and evaluated its anti-inflammatory effects through *in vitro* and *in silico* approaches (22).

Materials and Methods

Sampling and essential oil extraction

The rhizome of *Curcuma angustifolia* was collected on 09th January, 2022 from the Similipal Biosphere Reserve, Mayurbhanj district of Odisha, India (N 21°42'24.6", E 086° 21'45.7"). The plant was identified by Prof. PC Panda, Centre for Biotechnology, Siksha 'O' Anusandhan University. The voucher specimen (2526/CBT/21.01.2022) was stored in the Siksha 'O' Anusandhan University, Bhubaneswar, Odisha, India's herbarium. Hydro-distillation of 400 g of fresh *C. angustifolia* rhizome was carried out for 6 h using the Clevenger apparatus, adhering to the methodology outlined in the European Pharmacopoeia. The procedure was prolonged until no additional essential oil extraction was attainable. The essential oil was dehydrated with anhydrous sodium sulfate and kept at 4 °C until further experiments.

Analysis of essential oils through (GC-MS)

The phytochemical constituents in the extracted essential oil were identified utilizing a Clarus 580 gas chromatograph (GC) coupled with an SQ-8 mass spectrometry (MS) detector from Perkin-Elmer, USA. A splitless injection mode was employed, with 0.1 µL of undiluted essential oil injection. Separation was achieved using an Elite-5 MS capillary column (30 m x 0.25 mm I.D. x 0.25 µm).

The initial oven temperature was set to 60 °C. The temperature was further increased to 220 °C at 3 °C/min and fixed for 7 min at 220 °C. Furthermore, the transfer line injector temperatures had been fixed at 250 °C. The flow rate of helium was controlled at 1 mL/min and the electron ionization voltage was maintained at 70 eV. Compound percentages in the extracted essential oil were determined by integrating peak areas. Identification of compounds utilized mass spectrometry with the assistance of an integrated NIST library and comparison of experimental retention indices measured against straight-chain alkanes with literature retention indices.

Cell line maintenance

In this study, human ovarian teratocarcinoma pa-1 cells,

HCT 116 cells from human colorectal carcinoma as well as RAW 264.7 mouse monocyte/macrophage cells have been collected from NCCS, Pune, India. The HCT 116 cells and the pa1 cells have been developed in RPMI-1640 medium collected from Himedia and the cells were then supplemented with 10 % FBS that consists of an antibiotic mix of 0.1 % concentration. The antibiotic mix contained 10 mg/mL of streptomycin and penicillin of 10000 units. In contrast, RAW 264.7 cells underwent culture in DMEM high glucose media supplemented with 10 % FBS from Himedia, 1 % L Glutamine (200 mM) and 1 % antibiotic antimycotic solution. The cells were routinely continued at 37 °C in a humidified environment within a 5 % CO_2 incubator. Subsequent subculturing of these cells was performed every 48 h.

Cytotoxicity assay

The RAW 264.7 cells were treated using the above-mentioned method and were further cultured within the 96 culture plates which were incubated at 37 °C. After incubation, the cells were mixed with 6.25–100 µg/mL essential oil measuring 20 µL for 60 min. After this, a simulation was performed with lipopolysaccharides. The cells were incubated for 24 h and after the incubation period, 5 mg/mL MTT reagent, collected from HiMedia was added to each of the wells. These wells were further incubated for 60 min. After the incubation period, the supernatant was discarded. In the next step, 100 µL DMSO was poured into each of the wells. The quantification of the formazan crystals was done by implementing an ELISA plate reader at 540 nm.

In this study, 4 test compounds were analyzed to examine the cytotoxicity of the extracted *C. angustifolia* on the cell line named RAW 264.7. In order to conduct the assay, the concentrations that have been implemented in this study were documented.

Measurement of nitric oxide production

In this stage, the RAW 264.7 cells were cultured in 96 well plates. The plates were then incubated for 1 day for adherence. After that, the cells were stimulated with the essential oil (6.25–100 µg/mL) of *C. angustifolia*. After stimulation, the cells were incubated for 1 day at 37 °C. In this case, LPS can be used. After incubation, the 100 µL of the supernatant was collected. The supernatant was treated with a Griess reagent (100 µL), followed by absorbance measurement at 540 nm. The concentration of nitrite within the culture medium was determined by comparison with a standard curve of sodium nitrite.

Molecular docking study

Compounds sourced from *C. angustifolia* were obtained from the database PubChem (https://pubchem.ncbi.nlm.nih.gov/). Docking investigations concerning the compounds from *C. angustifolia* and iNOS (PDB ID: 6JWM) were conducted and assessed utilizing AutoDock Vina. iNOS was docked with the major compounds: 1,8-cineole, camphor, germacrene B, linalool, gamma-cadinene, beta-caryophyllene, neocurdione, germacrone, veleral and beta-elemene. The crystal structure of iNOS (PDB ID: 6JWM) was derived from the RCSB-PDB (https://www.rcsb.org/), and the compounds were also retrieved from PubChem database (https://pubchem.ncbi.nlm.nih.gov/).

ADME and toxicity properties prediction

The evaluation of absorption, distribution, metabolism, excretion (ADME) properties and drug-likeness assessment for the identified compounds encompassed an assessment of characteristics related to their distribution, absorption, metabolism and excretion. The drug-likeness attributes of the chosen compounds were assessed using the web server SwissADME (http://www.swissadme.ch/). The criteria for drug likeness included adherence to Lipinski's rule of 5 (23), the Egan rule (24) and Veber's rule (25).

To assess the potential toxicity of these phytochemical constituents, we used the online webserverProTox-II (https://tox-new.charite.de/protox_II/).

Desmond molecular dynamics simulation

Desmond package in SchrÖdinger suit (D. E. Shaw Research: Resources) was used for MD simulations. The ligand-protein complex selection was immersed in a 10 Å simple point charge (SPC) model and was employed for water box. Negatively charged particles were balanced by the incorporation of counter ions. To match the physiological conditions, a salt concentration of 0.15 M sodium and chloride ions was introduced. The NPT ensemble molecular dynamics (MD) was conducted at 300 K and 1.63 bar pressure for a duration of 50 ns, with energy recording at 1.2 ps intervals and trajectory recording every 50 ps. The OPLS-4 force field was used for MD simulations. Desmond simulation interaction diagram tool was used to create the graphical representations.

Statistical analysis

The data from the above-mentioned tests were expressed as mean ± SD. Using ANOVA, significant differences were calculated. The Turkey post hoc test was executed with a significance threshold set at $p<0.05$, employing GraphPad Prism version 8.0 (GraphPad Software Inc, California, USA).

Results and Discussion

Essential oil composition

In this study, we utilized the hydro-distillation technique to extract essential oil from fresh rhizomes of *Curcuma angustifolia*, of the Zingiberaceae family, sourced from the Similipal district of Odisha. The yield of essential oil obtained from *C. angustifolia* rhizomes was determined to be 0.6 % (v/w). The chemical components of *C. angustifolia* are displayed in Table 1. The entire 44 compounds were identified, representing 92.31 % of rhizome oil. According to a study, the oil yield of *C. angustifolia* rhizome was 0.4 % (v/w). A total of 35 compounds were identified, constituting 92 % of the rhizome oil (26). An author observed 0.8 and 0.014 % essential oil yields from *C. angustifolia* rhizomes from Jagdalpur, Madhya Pradesh (central India) and Travancore, Kerala, (South India) respectively (27). The extraction yield of the essential oil

from *C. angustifolia* exhibits variations attributed to geographical locations, genotypes and the season of collection. These factors are the primary contributors to the observed differences in essential oil composition.

In this study, 44 components, comprising 92.31 % of the total essential oil were identified using GC/MS analysis. On the Elite-5 MS column, the 44 phytochemical components are given in the order of their constituents (Table 1). Among the 44 compounds identified, the major constituents in the essential oil extracted from *C. angustifolia* rhizomes were velleral (17.82 %), germacrone (12.91 %), cryptomerione (11.52 %), curzerene (5.66 %), β-elemene (4.09 %), 1,8-Cineole (3.32 %), germacrone-B (2.77 %), β-caryophyllene (2.92 %), neocurdione (3.22 %) and γ-cadinene (2.69 %). The composition of this essential oil was predominantly characterized by oxygenated monoterpene (12.85 %), sesquiterpene hydrocarbons (19.19 %), monoterpene hydrocarbon (3.42 %) and oxygenated sesquiterpene (56.85 %). In a previous study, the primary constituents identified in the leaf oil of *C. angustifolia* included 8,9-dehydro-9-formyl-cycloisolongifolene (33.48 %), curzerenone (11.81 %), xanthorrhizol isomer (7.59 %), eucalyptol (6.62 %), camphor (3.27 %), germacrone (3.21 %), xanthorrhizol (2.98 %), ar-turmerone (1.62 %), curdione (1.60 %) and camphene (1.43 %).

Anti-inflammatory activities

The MTT assay was used to assess the viability of RAW 264.7 cells treated with *C. angustifolia* rhizome essential oil. Cells treated with various concentrations of essential oil (6.25–50 µg/mL) during a 24 h incubation period at 37 °C did not exhibit a significant decrease in viability compared to untreated cells. This observation contrasts with the findings of another study regarding the cytotoxic effects of turmeric extracts on RAW 264.7 cells, highlighting the diversity in research outcomes (28). However, our study found that *C. angustifolia* has moderate cytotoxicity potential, with an IC_{50} concentration of 111.43 µg/mL in cell cytotoxicity statistical data. Notably, *C. angustifolia* exhibited non-toxicity on RAW 264.7 cells up to a concentration of 50 µg/mL, where cell viability exceeded 70 %. This finding establishes 50 µg/mL as the optimum concentration for subsequent investigations (Fig. 1). Further exploration and analysis were performed to understand the underlying mechanisms and potential applications of *C. angustifolia* in cellular responses. Nitric oxide (NO) is considered to be a modulator of pathogenic processes, particularly acute inflammatory responses (29, 30). The investigation evaluated nitrite concentration in RAW 264.7 cells subsequent to treatment with LPS (1 µg/mL), both independently and in combination with different concentrations of *C. angustifolia* rhizome essential oil (6.25, 12.5 and 25 µg/mL). Incubation with rhizome essential oil demonstrated a dose-dependent decrease in LPS-induced nitrite production, as depicted in Fig. 2. This observed attenuation of nitrite production aligns with the anti-inflammatory potential of *C. angustifolia*, as reported in similar studies. For instance, the anti-inflammatory properties of certain plant-derived compounds, including

Table 1. Analyzing gas chromatography-mass spectrometry (GC-MS) data, we investigated the chemical composition of *Curcuma angustifolia* rhizome essential oil.

Sl. No.	RI_{exp}	RI_{Lit}	Compound	Peak area %
1	927	926	Tricyclene	0.48
2	943	954	Camphene	1.38
3	965	975	Sabinene	0.22
4	971	979	β-Pinene	0.49
5	981	990	Myrcene	0.24
6	1023	1029	Limonene	0.61
7	1028	1031	1,8-Cineole	3.32
8	1084	1090	2-Nonanone	0.12
9	1098	1096	Linalool	2.55
10	1144	1146	Camphor	3.64
11	1160	1160	Isoborneol	1.88
12	1167	1163	trans-β-Terpineol	0.43
13	1175	1188	α-Terpineol	0.40
14	1190	1199	γ-Terpineol	0.51
15	1327	1338	δ-Elemene	0.80
16	1366	1376	α-Copaene	0.11
17	1373	1390	β-Elemene	0.17
18	1383	1390	β-Elemene	4.10
19	1412	1419	β-caryophyllene	2.92
20	1420	1436	γ-Elemene	0.31
21	1439	1441	Aromadendrene	0.32
22	1445	1454	α-Humulene	0.94
23	1463	1498	Pseudowiddrene	0.19
24	1472	1513	γ-Cadinene	2.70
25	1479	1490	β-Selinene	0.67
26	1499	1500	Isodaucene	2.19
27	1508	1509	Germacrene-A	0.32
28	1518	1523	δ-Cadinene	0.67
29	1550	1561	Germacrene-B	2.78
30	1488	1499	Curzerene	5.66
31	1531	1535	10-epi-Cubebol	0.14
32	1579	1583	Caryophyllene oxide	0.40
33	1576	1590	Globulol	0.28
34	1588	1592	Viridiflorol	0.56
35	1596	1602	trans-β-Elemenone	0.18
36	1603	1607	5-epi-7-epi-α-Eudesmol	0.18
37	1611	1619	Junenol	1.39
38	1622	1627	2-epi-α-Cedren-3-one	0.75
39	1647	1660	Gymnomitrol	1.20
40	1674	1675	8-hydroxy-Isobornyl isobutanoate	0.60
41	1693	1693	Germacrone	12.92
42	1713	1724	Cryptomerione	11.53
43	1744	1693	Neocurdione	3.23
44	1791	1739	Velleral	17.83
			Monoterpene hydrocarbon	3.42 %
			Oxygenated monoterpene	12.85 %
			Sesquiterpene hydrocarbons	19.19 %
			Oxygenated sesquiterpene	56.85 %
			Total	92.31 %

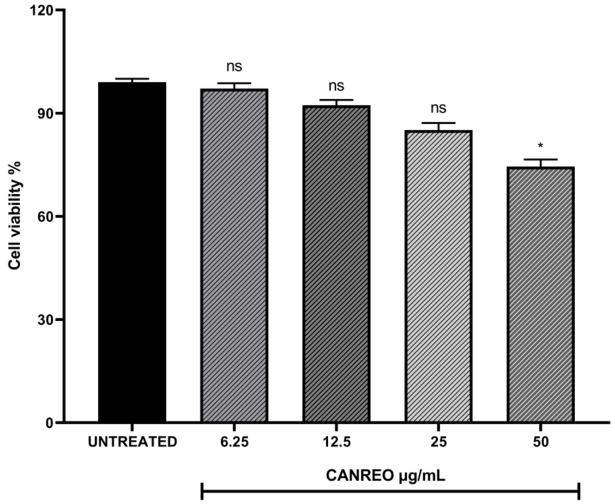

Fig. 1. *C. angustifolia* rhizome essential oils were evaluated for their impact on cell viability using RAW 264.7 cells. The cells were exposed to varying concentrations of essential oils (ranging from 6.25 to 50 µg/mL) for duration of 24 h. The methyl thiazolyl tetrazolium (MTT) assay was employed to determine the total number of viable cells. The results, presented as mean ± SD (n=3), indicated the control group (untreated cells) with a black bar. The statistical analysis encompassed a one-way analysis of variance, followed by the Tukey test, indicating significance levels denoted by * for p<0.05 and ** for p<0.01 between the control group and various concentrations of CANREO essential oils.

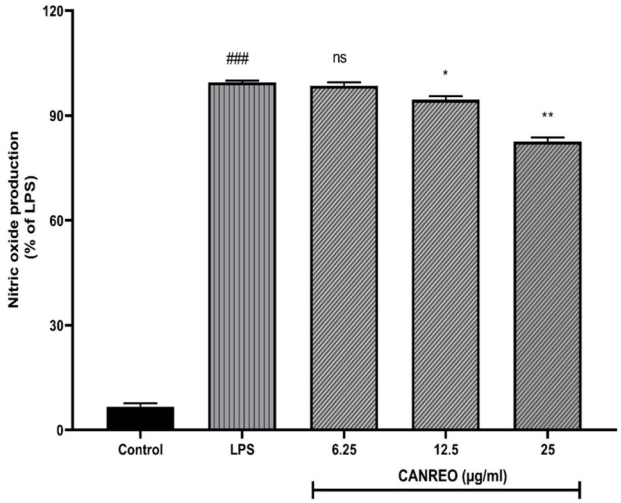

Fig. 2. Representation of the percentage of the total NO production that is observed in the essential oil with various concentrations treated on LPS-stimulated raw cells as well as essential oils, CAREO inhibited the total number of NO in a dose-dependent way till 25 µg/mL. Data are expressed as means ± standard deviation (SD) from 3 different experiments (n=3), with * indicating p<0.5 and ** indicating p<0.01, as compared with LPS ###p<0.001 LPS treated group compared with control.

essential oils, have been linked to their ability to modulate nitric oxide (NO) production (31, 32). The reduction in NO production, as indicated by the decrease from 100 % in LPS alone-induced cells to 66.42 % at the concentration of 25 µg/mL, underscores the potential of *C. angustifolia* rhizome essential oil in mitigating inflammatory responses.

Docking of the compounds from *C. angustifolia* to iNOS

Nitric oxide synthases (NOS) exist in 3 separate forms: neuronal NOS (nNOS), inducible NOS (iNOS) and endothelial NOS (eNOS). Among these, iNOS holds particular significance and is closely associated with inflammation. It serves a crucial function in controlling the amount of NO produced during inflammatory processes (33). The compounds velleral and germacrone inhibited iNOS enzyme more effectively than neocurdione and γ-cadinene. This observation prompted an investigation into the capability mechanism of NO inhibition and the interactions of these compounds with the iNOS protein through molecular docking (34, 35). *C. angustifolia* contained complex constituents that were not easy to understand with limited analyses and biological technologies. Ligand-protein interaction was predicted using molecular docking. The docked conformers of velleral, germacrone, neocurdione and γ-cadinene had the best predicted binding energy of -5.8, -5.4, -5.2 and -5.2 kcal/mol respectively (Table 2, Fig. 3). Therefore, the docking results suggested *C. angustifolia* exhibited anti-inflammatory effects via targeting the NF-κB pathways.

In silico ADME and toxicity assessment of ligands

Physicochemical characteristics being its potential as a drug development, we performed ADME studies. The ability to identify phytocompounds based on their drug-likeness would help us filter out those with less therapeutic importance. It was done by following Lipinski's rule of 5 (23), Egan's (24) and Veber's (25) rules.

Table 2. Docking results of compounds from *Curcuma angustifolia* (CA) with iNOS.

Ligand	PubChem CID	Binding affinity (Kcal/mol)	H-bond interactions	Other bond interactions
Velleral	CID_14412869	-5.8	GLN:157, GLN:160	PRO:153, ALA:154, LEU:187, GLY:158, LEU:161, THR:185
Germacrone	CID_6436348	-5.4	-	ALA:181, GLY:184, ILE:182, GLY:183, LEU:167, ARG:166, LEU:168, GLU:92, ARG:215, LEU:33, LEU:217
Neocurdione	CID_5316216	-5.2	GLY:183, ARG:166	PRO:164, ILE:182, LEU:167, GLY:184, GLU:92, LEU:168
γ-Cadinene	CID_15094	-5.2	-	ALA:154, GLY:158, PRO:153, LEU:161, GLN:157, LEU:187, THR:185
Germacrene_B	CID_5281519	-5.1	-	ARG:166, ALA:181, PRO:164, LEU:167, GLY:183, ILE:182, LEU:168, GLY:184, GLU:92, ARG:215
Curzerene	CID_572766	-5	-	GLY:184, LEU168, GLY:183, ARG:166, LEU:167, GLU:92, ARG:215, LEU:33, LEU:217
β-Elemene	CID_6918391	-4.9	-	GLY:184, LEU:33, LEU:168, LEU:217, PRO:37, ARG:215, GLY:184
β-Caryophyllene	CID_5281515	-4.7	-	GLN:157, THR:185, LEU:187, GLY:183, LEU:161, ILE:182, GLN:160

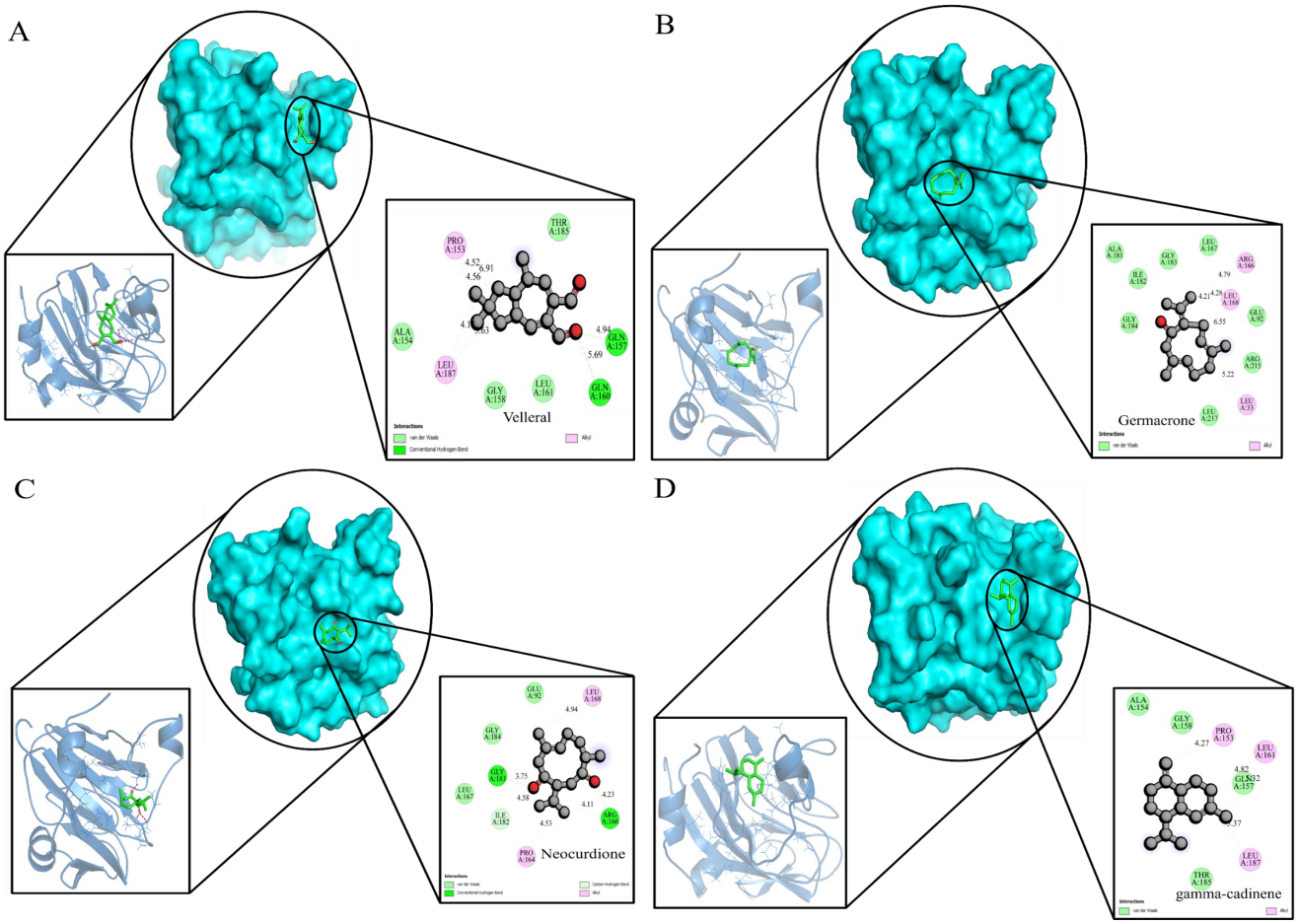

Fig. 3. Depicts the docking poses of Velleral (A), Germacrone (B), Neocurdione (C) and Gamma-Cadinene (D) at the substrate binding site of inducible nitric oxide synthases (iNOS). The different orientations and interactions of these phytocompounds at the active site are shown, providing information on their probable binding processes.

The criteria include a requirement for the molecular weight (MW) to be below 500, a topological surface area (TPSA) less than 140, lesser than 5 hydrogen bond acceptors (nOHNH), lesser than 5 hydrogen bond donors (nON) and lesser than 10 rotatable bonds (nrotb). According to these findings, all 8 selected compounds successfully complied with Lipinski's, Egan's and Veber's rules, indicating favorable druglike, leadlike and pharmacokinetic properties (Table 3). To determine the toxicity characteristics of the chosen phytocompounds, we used the ProTox-II web server (Table 4). The hypothesis posited that none of the selected compounds exhibited mutagenic, carcinogenic, immunotoxic or hepatotoxic properties. As the LD_{50} values of all of the chosen phytocompounds were greater than 2000 mg/kg, it can be inferred that these compounds are safe for biological administration and possess the potential for use as anti-inflammatory medications.

Table 3. SwissADME: Drug-likeness characteristics of the 8 compounds that qualifies with Lipinski's rule of 5, Veber's rule and the Egan rule.

Compounds	Lipinski	Veber	Egan	Abbott bioavailability score
Velleral	Yes	Yes	Yes	0.55
Germacrone	Yes	Yes	Yes	0.55
Neocurdione	Yes	Yes	Yes	0.55
γ-Cadinene	Yes	Yes	Yes	0.55
Germacrene_B	Yes	Yes	Yes	0.55
Curzerene	Yes	Yes	Yes	0.55
β-Elemene	Yes	Yes	Yes	0.55

Desmond package molecular dynamics

Docking provides a static representation of the binding poses of a molecule within the active site of the protein. On the other hand, molecular dynamic (MD) simulations prefer to calculate the atoms' moves with time by incorporating Newton's classical equation of motion (36). MD portrays the dynamic behavior of a molecular system, evaluating the stability of the interaction between a protein and ligand. The results from molecular docking demonstrated that *C. angustifolia* major components: velleral, germacrone, neocurdione and γ-cadinene interacting with iNOS were considered for molecular dynamics studies with the OPLS-4 force field. 5 systems iNOS protein and iNOS ligand complex (velleral-iNOS, germacrone-iNOS, neocurdione-iNOS and γ-cadinene-iNOS) were simulated in Desmond for 50 ns, since utilizing shorter simulation durations (<25 ns) might be deceptive and it would be difficult to discern between active and inactive ligands. This will aid our study of the binding stability of ligands inside the iNOS active site. Root-mean-square deviation (RMSD) values for protein backbones were calculated relative to their respective starting conformations in order to examine the dynamic stability of each system. With reference to the initial time frame of 0

Table 4. Protox-II: Prediction of toxicity evaluated with program Protox.

Compounds	Classification	Target	Prediction	Probability	Class
	Organ toxic	Hepatotoxic	Nonfunctional	0.68	5
	Toxicity end	Carcinogenic	Nonfunctional	0.57	
Velleral	Toxicity end	Immunotoxic	Nonfunctional	0.93	
	Toxicity end	Mutagenic	Nonfunctional	0.82	
	Toxicity end	Cytotoxic	Nonfunctional	0.82	
	Organ toxic	Hepatotoxic	Nonfunctional	0.71	5
	Toxicity end	Carcinogenic	Nonfunctional	0.77	
Germacrone	Toxicity end	Immunotoxic	Nonfunctional	0.98	
	Toxicity end	Mutagenic	Nonfunctional	0.85	
	Toxicity end	Cytotoxic	Nonfunctional	0.9	
	Organ toxic	Hepatotoxic	Nonfunctional	0.71	5
	Toxicity end	Carcinogenic	Nonfunctional	0.69	
Neocurdione	Toxicity end	Immunotoxic	Functional	0.61	
	Toxicity end	Mutagenic	Nonfunctional	0.86	
	Toxicity end	Cytotoxic	Nonfunctional	0.9	
	Organ toxic	Hepatotoxic	Nonfunctional	0.84	5
	Toxicity end	Carcinogenic	Nonfunctional	0.76	
γ-Cadinene	Toxicity end	Immunotoxic	Functional	0.55	
	Toxicity end	Mutagenic	Nonfunctional	0.69	
	Toxicity end	Cytotoxic	Nonfunctional	0.74	
	Organ toxic	Hepatotoxic	Nonfunctional	0.81	5
	Toxicity end	Carcinogenic	Nonfunctional	0.75	
Germacrene_B	Toxicity end	Immunotoxic	Nonfunctional	0.98	
	Toxicity end	Mutagenic	Nonfunctional	0.86	
	Toxicity end	Cytotoxic	Nonfunctional	0.83	
	Organ toxic	Hepatotoxic	Nonfunctional	0.74	4
	Toxicity end	Carcinogenic	Nonfunctional	0.54	
Curzerene	Toxicity end	Immunotoxic	Nonfunctional	0.99	
	Toxicity end	Mutagenic	Nonfunctional	0.8	
	Toxicity end	Cytotoxic	Nonfunctional	0.81	
	Organ toxic	Hepatotoxic	Nonfunctional	0.79	5
	Toxicity end	Carcinogenic	Nonfunctional	0.72	
β-Elemene	Toxicity end	Immunotoxic	Nonfunctional	0.99	
	Toxicity end	Mutagenic	Nonfunctional	0.76	
	Toxicity end	Cytotoxic	Nonfunctional	0.83	

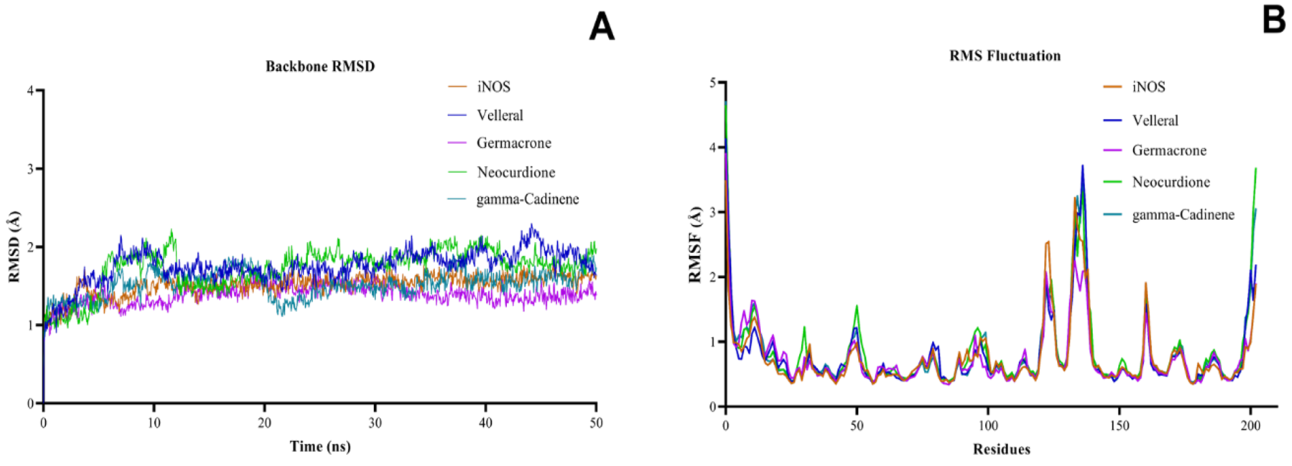

Fig. 4. Depicts the Desmond RMSD values, which represent fluctuations in protein backbones throughout the period of the simulation. The RMSF profile of the C-α atom provides insight into the dynamic behavior of certain chemical structures in the researched systems. These metrics give useful information on the stability and flexibility of protein structures during molecular dynamics simulations.

ns, all systems simulated attained equilibrium after 25 ns, as seen in Fig. 4. Average RMSD for the backbone protein was less than 2.5 Å, indicating a consistent trend in RMSD up to 50 ns. All of the fluctuations were below the allowable range of 3 Å, thus they are negligible. To infer any localized changes in iNOS complexes following the binding of phytocompounds relative to protein, we presented the root mean square fluctuation (RMSF) profile of the C-α atom for all systems, offering insights into the dynamic behavior of the molecular structures under investigation. The amino acid residues associated in contact with the compounds exhibited minor fluctuations. The RMSF of iNOS protein-complex amino acids varied from 0.7 to 3.85 Å. When compared to the iNOS-Germacrone complex and protein, the iNOS-Velleral, iNOS-Neocurdione, and iNOS-gamma-Cadinene showed slightly high fluctuations. Meanwhile, the iNOS amino acid-phytocompound interaction was time-resolved to 50 ns to build an interaction potential map. The X-axis shows the interacting amino acid residues, while the Y-axis displays the interaction fraction (Fig. 5). Slight tweaks to the phytocompound-iNOS interaction were noted during simulation, but the essential interaction observed during docking in the docked-ligand constituents did not change. The robust interaction between the ligand and the protein is not solely attributed to hydrogen bonding; it can also result from hydrophobic interactions, ionic interactions and the formation of salt bridges. The stability of the contact and the conformational changes at various times of the simulation were shown by the interaction of MD trajectories. Although molecular docking is a quick and effective method for determining the binding position of a ligand within a protein's active site, it does not account for the conformational changes that may occur in the protein as a result of ligand interaction (37). Likewise, the study demonstrated the examination of MD trajectories, encompassing the assessment of interaction stability and conformational changes at different intervals throughout the MD simulation. The MD stability of an individual complex can be evaluated by computing the protein's backbone RMSD based on its initial conformation. Interaction of phytocompounds with iNOS receptors did not cause local alterations based on the RMSF pattern of the C-atom across all systems. Four compounds were identified showing consistent interaction with the protein, suggesting they may be promising therapeutic candidates for the treatment of inflammatory disorders.

Conclusion

The anti-inflammatory potential of the *Curcuma angustifolia* species was determined using *in vitro* and *in silico* studies. The GC-MS analysis was used to identify the compounds in *C. angustifolia* essential oil. The investigation showcased the inhibitory capabilities of bioactive elements present in the essential oil of *C. angustifolia* against iNOS, employing computational methodologies. The *C. angustifolia*-derived velleral, germacrone, neocurdione, and γ-cadinene were the lead chemicals having iNOS inhibiting ability. All-atom MD simulations on 4 phytocompounds revealed a significant binding site of iNOS and induced a conformational shift, allowing ligands to reposition within the binding interface. This computational study represents the initial exploration aimed at identifying 4 potential bioactive compounds with higher binding affinity to iNOS. Further *in vivo* validation is necessary to ascertain the potential of these novel compounds as anti-inflammatory drugs for human inflammatory diseases.

Acknowledgements

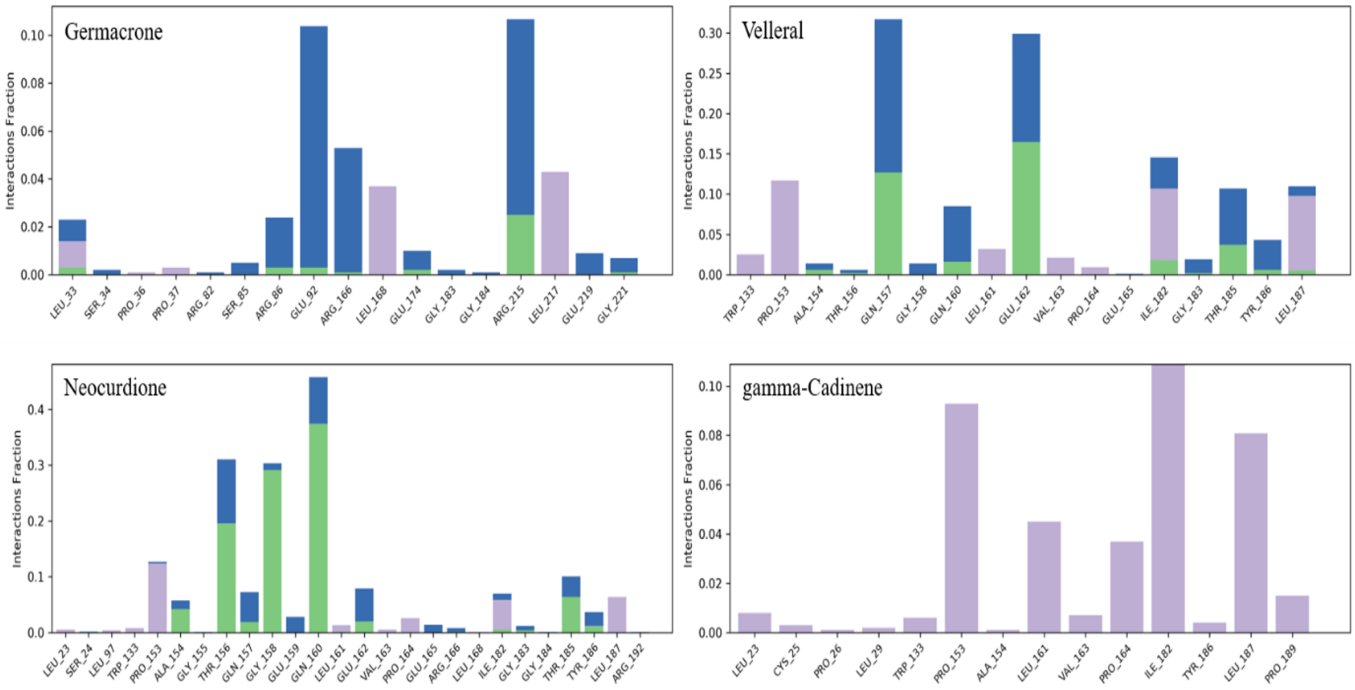

Fig. 5. Bar graph shows the interacting residues of germacrone, velleral, neocurdione and γ-cadinene interact with iNOS, while several connections were altered throughout the simulation. These contacts are stable due to not just hydrogen bonding, but also hydrophobic, ionic and salt bridge interactions.

The authors express gratitude to President Manoj Ranjan Nayak of Siksha 'O' Anusandhan Deemed to be University and to the Dean of the School of Pharmaceutical Sciences for their support in providing infrastructure and fruitful laboratory resources.

Authors' contributions

Conceptualization: SN and AG; Methodology: AG and AN; Formal analysis: AG, AN, SJ and AR; Data curation: AG and AN; Visualization: AG; Writing original draft preparation: AR, PCP and SN; Writing review and editing: AG, AN, AS, SJ, PCP, AR and SN; Supervision: SN. All authors have read and agreed to the final version of the manuscript.

Compliance with ethical standards

Conflict of interest: Authors do not have any conflict of interests to declare.

Ethical issues: None.

References

1. Azab A, Nassar A, Azab AN. Anti-inflammatory activity of natural products. Molecules. 2016;21:1321. https://doi.org/10.3390/molecules21101321
2. Saleem TM, Azeem AK, Dilip C, Sankar C, Prasanth NV, Duraisami R. Anti–inflammatory activity of the leaf extracts of *Gendarussa vulgaris* Nees. Asian Pac J Trop Biomed. 2011;1:147-49. https://doi.org/10.1016/S2221-1691(11)60014-2
3. García-Aranda MI, Gonzalez-Padilla JE, Gómez-Castro CZ, Gómez-Gómez YM, Rosales-Hernández MC, et al. Anti-inflammatory effect and inhibition of nitric oxide production by targeting COXs and iNOS enzymes with the 1, 2-diphenylbenzimidazole pharmacophore. Bioorg Med Chem. 2020;28:115427. https://doi.org/10.1016/j.bmc.2020.115427
4. Venkata M, Sripathy R, Anjana D, Somashekara N, Krishnaraju A, Krishanu S, et al. *In silico*, *in vitro* and *in vivo* assessment of safety and anti-inflammatory activity of curcumin. Am J Infect Dis. 2012;8:26. https://doi.org/10.3844/ajidsp.2012.26.33
5. Jamali T, Kavoosi G, Jamali Y, Mortezazadeh S, Ardestani SK. *In-vitro*, *in-vivo* and *in-silico* assessment of radical scavenging and cytotoxic activities of *Oliveria decumbens* essential oil and its main components. Sci Rep. 2021;11:14281. https://doi.org/10.1038/s41598-021-93535-8
6. Javaid A, Chaudhury FA, Khan IH, Ferdosi MFH. Potential health-related phytoconstituents in leaves of *Chenopodium quinoa.* Adv Life Sci. 2022;9(4):574-78.
7. Javaid A, Khan IH, Ferdosi MFH, Manzoor M, Anwar A. Medically important compounds in *Ipomoea carnea* flowers. Pak J Weed Sci Res. 2023;29(2):115-21. https://dx.doi.org/10.17582/journal.PJWSR/2023/29.2.115.121
8. Ibáñez MD, Blázquez MA. *Curcuma longa* L. rhizome essential oil from extraction to its agri-food applications. A review. Plants. 2020;10:44. https://doi.org/10.3390/plants10010044
9. Verma RK, Kumari P, Maurya RK, Kumar V, Verma RB, Singh RK. Medicinal properties of turmeric (*Curcuma longa* L.): A review. Int J Chem Stud. 2018;6:1354-57.
10. Jena S, Ray A, Sahoo A, Kar B, Panda PC, Nayak S. Chemical constituents of leaf essential oil of *Curcuma angustifolia* Roxb. growing in eastern India. J Essent Oil-Bear Plants. 2016;19:1527-31. https://doi.org/10.1080/0972060X.2016.1250677
11. Akinola OS, Irekhore OT, Ademolue RO. Evaluation of growth, reproductive performance and economic benefits of rabbits fed diets supplemented with turmeric (*Curcuma longa*) powder. Egypt Poult Sci J. 2020;40:701-14. https://doi.org/10.21608/epsj.2020.115968
12. Umar NM, Parumasivam T, Aminu N, Toh SM. Phytochemical and pharmacological properties of *Curcuma aromatica* Salisb (wild turmeric). J Appl Pharm Sci. 2020;10:180-94.
13. Sharma S, Ghataury SK, Sarathe A, Dubey G, Parkhe G. *Curcuma angustifolia* Roxb. (Zingiberaceae): Ethnobotany, phytochemistry and pharmacology: A review. J Pharmacogn Phytochem. 2019;8:1535-40.
14. Singh SS. Cultivation practices of *Curcuma angustifolia* Roxb. ICAR Research Complex for NEH Region, Manipur Centre, Lamphelpat, Imphal, India. Int J Agric Sci. ISSN. 2021:0975-3710.
15. Bonacina C, da Cruz RM, Nascimento AB, Barbosa LN, Gonçalves JE, Gazim ZC, Magalhaes HM, de Souza SG. Salinity modulates growth, oxidative metabolism and essential oil profile in *Curcuma longa* L. (Zingiberaceae) rhizomes. S Afr J Bot. 2022;146:1-1. https://doi.org/10.1016/j.sajb.2021.09.023
16. Dosoky NS, Setzer WN. Chemical composition and biological activities of essential oils of *Curcuma* species. Nutrients. 2018;10:1196. https://doi.org/10.3390/nu10091196
17. Chanda S, Ramachandra TV. Phytochemical and pharmacological importance of turmeric (*Curcuma longa*): A review. Research and Reviews: J Pharmacol. 2019;9:16-23.
18. Javed S, Mehmood Z, Javaid A, Javaid A. Biocidal activity of citrus peel essential oils against some food spoilage bacteria. J Med Plants Res. 2011;5(16): 2868-72.
19. Ferdosi MFH, Khan IH, Javaid A. Composition of essential oil isolated from marigold (*Tagetes erecta* L.) flowers cultivated in Lahore, Pakistan. Bangladesh J Bot. 2022;51(4): 683-88. https://doi.org/10.3329/bjb.v51i4.63486
20. Setzer WN, Duong L, Poudel A, Mentreddy SR. Variation in the chemical composition of five varieties of *Curcuma longa* rhizome essential oils cultivated in North Alabama. Foods. 2021;10:212. https://doi.org/10.3390/foods10020212
21. Nayak S, Jena, AK, Sucharita S. *In vitro* bioactivity studies of wild *Curcuma angustifolia* rhizome extract against (HeLa) human cervical carcinoma cells. World Journal of Pharmacy and Pharmaceutical Sciences. 2013;2:4972-86.
22. Gadnayak A, Dehury B, Nayak A, Jena S, Sahoo A, Panda PC, et al. Mechanistic insights into 5-lipoxygenase inhibition by active principles derived from essential oils of *Curcuma* species: Molecular docking, ADMET analysis and molecular dynamic simulation study. PloS One. 2022;17:e0271956. https://doi.org/10.1371/journal.pone.0271956
23. Lipinski CA. Poor aqueous solubility-an industry wide problem in drug discovery. Am Pharm Rev. 2002;5:82-85.
24. Egan WJ. Predicting ADME properties in drug discovery. Drug design: structure-and ligand-based approaches. Cambridge University Press. 2010:165-77. https://doi.org/10.1017/CBO9780511730412.013
25. Pollastri MP. Overview on the rule of five. Current Protocols in Pharmacology. 2010;49:9-12. https://doi.org/10.1002/0471141755.ph0912s49
26. Jena S, Ray A, Banerjee A, Sahoo A, Nasim N, Sahoo S, et al. Chemical composition and antioxidant activity of essential oil from leaves and rhizomes of *Curcuma angustifolia* Roxb. Nat Prod Res. 2017;31:2188-91. https://doi.org/10.1080/14786419.2017.1278600
27. Srivastava AK, Srivastava SK, Syamsundar KV. Volatile composition of *Curcuma angustifolia* Roxb. rhizome from central and southern India. Flavour Fragr J. 2006;21:423-26. https://doi.org/10.1002/ffj.1680

28. Gouthamchandra K, Sudeep HV, Chandrappa S, Raj A, Naveen P, Shyamaprasad K. Efficacy of a standardized turmeric extract comprised of 70 % bisdemothoxy-curcumin (REVERC3) against LPS-induced inflammation in RAW264. 7 cells and carrageenan-Induced paw edema. J Inflamm Res. 2021;14:859. https://doi.org/10.2147/JIR.S291293

29. Ricciardolo FL, Sterk PJ, Gaston B, Folkerts G. Nitric oxide in health and disease of the respiratory system. Physiol Rev. 2004;84:731-65. https://doi.org/10.1152/physrev.00034.2003

30. Ray A, Jena S, Sahoo A, Kamila PK, Das PK, Mohanty S, et al. Chemical composition, antioxidant, anti-inflammatory and anticancer activities of bark essential oil of *Cryptocarya amygdalina* from India. J Essent Oil-Bear Plants. 2021;24:617-31. https://doi.org/10.1080/0972060X.2021.1950051

31. Schmitt CA, Dirsch VM. Modulation of endothelial nitric oxide by plant-derived products. Nitric Oxide. 2009;21:77-91. https://doi.org/10.1016/j.niox.2009.05.006

32. de Cássia da Silveira e Sá R, Andrade LN, de Sousa DP. A review on anti-inflammatory activity of monoterpenes. Molecules. 2013;18:1227-54. https://doi.org/10.3390/molecules18011227

33. Garcin ED, Arvai AS, Rosenfeld RJ, Kroeger MD, Crane BR, Andersson G, et al. Anchored plasticity opens doors for selective inhibitor design in nitric oxide synthase. Nat Chem Biol. 2008;4:700-07. https://doi.org/10.1038/nchembio.115

34. Xu J, Peng M, Sun X, Liu X, Tong L, Su G, et al. Bioactive diterpenoids from *Trigonostemon chinensis*: structures, NO inhibitory activities and interactions with iNOS. Bioorg Med Chem Lett. 2016;26:4785-89. https://doi.org/10.1016/j.bmcl.2016.08.026

35. Chayah M, Carrión MD, Gallo MA, Jiménez R, Duarte J, Camacho ME. Development of urea and thiourea kynurenamine derivatives: synthesis, molecular modeling and biological evaluation as nitric oxide synthase inhibitors. Chem Med Chem. 2015;10:874-82. https://doi.org/10.1002/cmdc.201500007

36. Eftekhari SA, Toghraie D, Hekmatifar M, Sabetvand R. Mechanical and thermal stability of armchair and zig-zag carbon sheets using classical MD simulation with Tersoff potential. Phys. E: Low-Dimens. Syst Nanostructures. 2021;133:114789. https://doi.org/10.1016/j.physe.2021.114789